Acta Oceanol. Sin., 2018, Vol. 37, No. 7, P. 131–140
DOI: 10.1007/s13131-018-1250-0
http://www.hyxb.org.cn
E-mail: hyxbe@263.net

Vessel fusion tracking with a dual-frequency high-frequency surface wave radar and calibrated by an automatic identification system

ZHANG Hui[1, 2], LIU Yongxin[2]*, JI Yonggang[3], WANG Linglin[1]

[1] College of Computer Science, Inner Mongolia University, Hohhot 010021, China

[2] College of Electronic Information Engineering, Inner Mongolia University, Hohhot 010021, China

[3] The First Institute of Oceanography, State Oceanic Administration, Qingdao 266061, China

Received 26 August 2017; accepted 27 September 2017

Abstract

High-frequency surface wave radar (HFSWR) and automatic identification system (AIS) are the two most important sensors used for vessel tracking. The HFSWR can be applied to tracking all vessels in a detection area, while the AIS is usually used to verify the information of cooperative vessels. Because of interference from sea clutter, employing single-frequency HFSWR for vessel tracking may obscure vessels located in the blind zones of Bragg peaks. Analyzing changes in the detection frequencies constitutes an effective method for addressing this deficiency. A solution consisting of vessel fusion tracking is proposed using dual-frequency HFSWR data calibrated by the AIS. Since different systematic biases exist between HFSWR frequency measurements and AIS measurements, AIS information is used to estimate and correct the HFSWR systematic biases at each frequency. First, AIS point measurements for cooperative vessels are associated with the HFSWR measurements using a JVC assignment algorithm. From the association results of the cooperative vessels, the systematic biases in the dual-frequency HFSWR data are estimated and corrected. Then, based on the corrected dual-frequency HFSWR data, the vessels are tracked using a dual-frequency fusion joint probabilistic data association (JPDA)-unscented Kalman filter (UKF) algorithm. Experimental results using real-life detection data show that the proposed method is efficient at tracking vessels in real time and can improve the tracking capability and accuracy compared with tracking processes involving single-frequency data.

Key words: vessel tracking, high-frequency surface wave radar, automatic identification system, joint probabilistic data association, unscented Kalman filter

Citation: Zhang Hui, Liu Yongxin, Ji Yonggang, Wang Linglin. 2018. Vessel fusion tracking with a dual-frequency high-frequency surface wave radar and calibrated by an automatic identification system. Acta Oceanologica Sinica, 37(7): 131–140, doi: 10.1007/s13131-018-1250-0

1 Introduction

Marine surveillance is a significant activity in the management of an exclusive economic zone (EEZ), and the assessment of illegal vessels is the primary task of maritime surveillance. There are two main sensors used for vessel tracking surveillance of large marine areas: automatic identification system (AIS) and high-frequency surface wave radar (HFSWR). The AIS is designed to avoid vessel collisions and can provide accurate information on cooperative vessels, i.e., the vessel position, length, width, velocity and heading. However, not all vessels are equipped with the AIS. Vessels with operable AIS equipment are usually defined as cooperative vessels, while others are non-cooperative vessels (Ji et al., 2014a). The HFSWR, which is exploited in a frequency band of 3–30 MHz, can detect and track vessels by differentiating between the echoes from vessels and the ocean caused by different Doppler shifts (Ponsford and Wang, 2010). The HFSWR is advantageous because it can offer continuous time surveillance capacity and direct the velocity estimations and has a long range (Grosdidier et al., 2010; Maresca et al., 2014). However, the HFSWR has a low spatial resolution (Gurgel et al., 2010).

In recent years, several algorithms for vessel detection and tracking using the HFSWR have been developed (Braca et al., 2015). Dzvonkovskaya et al. (2008, 2010) proposed a statistical method to analyze the HFSWR detection capacity for various vessel types. HFSWR systems are characterized by a poor azimuthal resolution, a high nonlinearity, and a significant false alarm rate. A joint probabilistic data association (JPDA) technology with the unscented Kalman filter (UKF) was proposed for vessel tracking (Braca et al., 2012). The JPDA method is a measurement-to-track association algorithm that has been proven valid for the tracking of multiple targets in a cluttered environment (Bar-Shalom and Li, 1995). The UKF is usually used to estimate the state of a target in a nonlinear system (Xiong et al., 2006). Maresca et al. (2014) proposed a vessel tracking method using multiple radars, and data fusion technology has been applied to improving the tracking performance. In the above mentioned works, AIS measurements are only used as the ground truth to validate the vessel target.

The dual-frequency HFSWR is often used to suppress the effects of sea clutter (Ji et al., 2014b). The sea clutter represents the

Foundation item: The National Natural Science Foundation of China under contract No. 61362002; the Marine Scientific Research Special Funds for Public Welfare of China under contract No. 201505002.
*Corresponding author, E-mail: yxliu@imu.edu.cn

returns from the sea during target detection processing. Bragg peaks, which are caused by the resonant interaction of HFSWR signals with waves, usually submerge the vessel returns with the surrounding returns (Ince et al., 1998). Therefore, Bragg peaks can generate blind velocity zones, and vessels that fall into these zones cannot be distinguished. Detecting frequency changes constitutes one of the more effective methods for overcoming this deficiency. A vessel that falls into the blind zone of a particular frequency can be detected at another frequency. Therefore, the vessel detection with dual-frequency data can improve the vessel tracking capability. Ji et al. (2016) proposed a vessel target detection algorithm based on fused range-Doppler (RD) images for the dual-frequency HFSWR. In this work, the dual-frequency data are fused at the RD-image level to obtain more reliable association results.

Some fusion algorithms have been proposed with AIS and radar measurements. In the work of Habtemariam et al. (2015), a measurement-level fusion algorithm was proposed to combine radar and AIS data in which radar measurements are utilized to update the AIS ID probabilities because of the uncertainties in the AIS ID-to-tracking capability. Vivone et al. (2015) proposed a knowledge-based multi-target vessel tracking method for the HFSWR in which AIS information is applied to providing prior information for sea lanes. Different dynamic models are used for the tracking according as whether vessels are within sea lanes. In these fusion algorithms, AIS measurements can provide some prior knowledge for the vessels and sea lanes.

To make use of prior AIS knowledge, the transformation of the AIS and HFSWR data into a standard reference system is a prerequisite process for the fusion of multiple-sensor systems (Zhou et al., 1997). Measurement biases may exist between various sensor systems, and many sensor registration algorithms have been proposed to compensate for these systematic errors (Zhou et al., 1997 , 1999; Bruno et al., 2013). Zhou et al. (1999) proposed a registration algorithm in an earth-centered earth-fixed (ECEF) coordinate system, and a least squares (LS) method was used to estimate the systematic errors between two radar systems. Bruno et al. (2013) proposed a theoretical analysis for HFSWR systematic biases for a comparison with AIS data.

In this study, our goal is to track vessels using the dual-frequency HFSWR and AIS measurements. Since different systematic biases exist between the HFSWR frequency measurements and AIS measurements, AIS information is used to estimate and correct the HFSWR systematic bias at each frequency. The AIS provides measurements in the world geodetic system 1984 (WGS84) reference datum, while the HFSWR provides measurements in radar station polar coordinates. The AIS measurements are transformed into the radar station polar coordinates, and the systematic biases between the AIS and dual-frequency HFSWR measurements are estimated with an iterative method. Following the compensation of the HFSWR systematic biases, vessels are tracked with a data fusion JPDA-UKF tracking algorithm with the dual-frequency HFSWR measurements.

The rest of the paper is organized as follows: Section 2 introduces vessel dynamic and measurement models; Section 3 presents a method used to estimate the HFSWR systematic biases with the association results of cooperative vessels; Section 4 proposes a new fusion JPDA-UKF tracking method for the dual-frequency HFSWR; Section 5 provides experimental results using real-life detection data; and finally, the conclusions are drawn in the Section 6.

2 Vessel dynamic and measurement models

The AIS provides measurements in the World Geodetic System 1984 (WGS84) reference datum, while HFSWR provides measurements in the radar station polar coordinates. To simplify the measurement system, the AIS measurements are transformed into the radar station polar coordinates, after which a dynamic model is established in the Cartesian coordinate system.

2.1 *Vessel dynamic model*

The vessel dynamic model at a time k is defined in the Cartesian coordinate system as follows:

$$\boldsymbol{X}_k = \boldsymbol{F}_k \boldsymbol{X}_{k-1} + \boldsymbol{Q}_k, \tag{1}$$

where $\boldsymbol{X}_k = [x_k \;\; \vec{x}_k \;\; y_k \;\; \vec{y}_k]^{\mathrm{T}}$, x_k and y_k are the position values along the x-axis and y-axis, respectively, $\vec{x}_k$ and $\vec{y}_k$ are the velocity vectors along the x-axis and y-axis, respectively; and $\boldsymbol{Q}_k$ is the processing noise. It is assumed that the vessel is moving with a uniform velocity along a straight line during the sampling time interval. Therefore, the state transition matrix $\boldsymbol{F}_k$ is defined as follows:

$$F_k = \begin{bmatrix} 1 & T_k & 0 & 0 \\ 0 & 1 & 0 & 0 \\ 0 & 0 & 1 & T_k \\ 0 & 0 & 0 & 1 \end{bmatrix}, \tag{2}$$

where T_k is the sampling time interval.

2.2 *Measurement model*

2.2.1 *HFSWR measurement model*

The HFSWR detects vessel targets continuously. The HFSWR measurement model is given by

$$\boldsymbol{z}_k^{\mathrm{h}} = H(X_k) + \boldsymbol{\Delta}_k + \boldsymbol{w}_k^{\mathrm{h}}, \tag{3}$$

where $\boldsymbol{\Delta}_k$ is the radar systematic bias, which contains the systematic biases in the range, azimuth and radial velocity; $\boldsymbol{w}_k^h$ is the HFSWR measurement noise, which is assumed to be zero-mean white Gaussian noise; and $H(X_k) = [r_k \;\; \theta_h \;\; u_k]^{\mathrm{T}}$, is the measurement function of the HFSWR, r_k is the range, θ_k is the azimuth, and υ_k is the radial velocity. The measurement equations are listed as follows:

$$\left.\begin{aligned} r_k\sqrt{(x_k - x_s)^2 + (y_k - y_s)^2} \\ \theta = \tan^{-1}\left(\frac{y_s - y_k}{x_s - x_k}\right) \\ \upsilon k = \frac{(x_k - x_s)\vec{x}_k + (y_k - y_s)\vec{y}_k}{\sqrt{(x_k - x_s)^2 + (y_k - y_s)^2}} \end{aligned}\right\}. \tag{4}$$

where x_{s} and y_{s} describe the positions of the radar stations. The covariance matrix is defined as follows:

$$\boldsymbol{R}_h = \begin{bmatrix} \sigma_r^2 & 0 & 0 \\ 0 & {\sigma_\theta}^2 & 0 \\ 0 & 0 & \sigma_v^2 \end{bmatrix}. \tag{5}$$

2.2.2 *AIS measurement model*

The time intervals between the AIS measurement reports depend on the types of AIS equipment and the dynamic state of the

vessel (Xiao et al., 2015; Habtemariam et al., 2015). Thus, the AIS measurement model is defined as follows:

$$z_k^{\mathrm{a}} = \begin{cases} G\left(X_k\right) + \boldsymbol{w}_k^{\mathrm{a}} & k = t_{\mathrm{re}}^m \\ \boldsymbol{Dr}\left(X_k\right) & t_{\mathrm{re}}^m < k < t_{\mathrm{re}}^{m+1} \end{cases}, \tag{6}$$

where $\boldsymbol{G}(\boldsymbol{X}_k)=\left[\begin{array}{cc} x_k & y_k \end{array}\right]^{\mathrm{T}}$ is a measurement function of the AIS; and $\boldsymbol{Dr}(\boldsymbol{X}_k)$ is the dead reckoning (DR) function. If the sampling time k equals the mth AIS report time t_{re}^m, the AIS measurements are directly provided by the AIS reports. If not, the DR method is employed to predict the AIS position and velocity from the AIS reports (Chaturvedi et al., 2012). Herein, it is assumed that there are no false alarms or missed detections using the AIS measurements and that the measurement noise $\boldsymbol{w}_k^{\mathrm{a}}$.

3 HFSWR systematic bias estimation based on information of cooperative vessels

Cooperative vessels can provide static and dynamic AIS information and can be simultaneously detected using HFSWR. The measurement errors in the AIS are negligible compared with those in the HFSWR. Thus, AIS information is treated as real information of cooperative targets. Different systematic biases exist between the HFSWR frequency measurements and the AIS measurements. In this section, AIS information is used to estimate the HFSWR systematic biases at each frequency. First, the HFSWR and AIS measurements of cooperative target are associated with the JVC algorithm. Then, the HFSWR systematic biases are estimated based on the association results.

3.1 *HFSWR and AIS point target association of cooperative vessels*

3.1.1 *Coordinate transformation*

The AIS measurements are defined in the WGS84 datum. The positions of the AIS measurements in latitude-longitude coordinates $(\zeta_{\mathrm{a}}, \lambda_{\mathrm{a}})$ are transformed into radar station polar coordinates (r_k, θ_k) as follows:

$$\left.\begin{aligned} r_k = R\arccos & \left[\begin{array}{l} \cos\left(90-\zeta_{\mathrm{a}}\right)\cos\left(90-\zeta_{\mathrm{s}}\right)+ \\ \sin\left(90-\zeta_{\mathrm{a}}\right)\sin\left(90-\zeta_{\mathrm{s}}\right)\cos\left(\lambda_{\mathrm{a}}-\lambda_{\mathrm{s}}\right)\end{array}\right] \\ \theta_k = \arcsin & \left[\cos\zeta_{\mathrm{a}}\frac{\sin\left(\lambda_{\mathrm{a}}-\lambda_{\mathrm{s}}\right)}{\sin\varphi_{\mathrm{s}}}\right] \end{aligned}\right\}, \tag{7}$$

where the position $(\zeta_{\mathrm{s}}, \lambda_{\mathrm{s}})$ denotes the geographical coordinate pair of the radar station, R is the radius of the earth; and φ_{s} is defined as follows:

$$\varphi_{\mathrm{s}} = \sin\zeta_{\mathrm{a}}\sin\zeta_{\mathrm{s}} + \cos\zeta_{\mathrm{a}}\cos\zeta_{\mathrm{s}}\times\cos\left(\lambda_{\mathrm{a}}-\lambda_{\mathrm{s}}\right). \tag{8}$$

The radial velocity of an AIS measurement is obtained through a conversion from course over ground (COG) θ_{cog} and speed over ground (SOG) v_{sog} data by

$$v_k = -v_{\mathrm{sog}}\times\cos\left(\theta-\theta_{\mathrm{cog}}\right). \tag{9}$$

The parameter v_k is a positive number when a vessel sails towards the radar station, whereas v_k is a negative number when a vessel sails away from the station.

3.1.2 *Measurement partition*

To apply the JVC algorithm, we first divide the complete set into many different combinations. Every combination contains all of the possible association measurements from both the AIS and HFSWR. A pair gating method is used to find the feasible associated target measurements between each pair of sensors. Furthermore, an iterative search method is employed to ensure that the divided combinations cover all of the possible associated target measurements.

The gating thresholds between the AIS and HFSWR measurements are given by

$$\left.\begin{aligned} \left|z_k^{\mathrm{h}}(r) - z_k^{\mathrm{a}}(r)\right| &\leqslant r_{\max} \\ \left|z_k^{\mathrm{h}}(\theta) - z_k^{\mathrm{a}}(\theta)\right| &\leqslant \theta_{\max} \\ \left|z_k^{\mathrm{h}}(v) - z_k^{\mathrm{a}}(v)\right| &\leqslant v_{\max} \end{aligned}\right\}, \tag{10}$$

where $r_{\max}$, $\theta_{\max}$ and $v_{\max}$ are the range, azimuth and radial velocity gating thresholds for the HFSWR and AIS measurements, respectively. These three gating thresholds correspond to the accuracy of the HFSWR detection results, and the accuracy is related to the HFSWR resolution. The HFSWR range resolution, which is determined by the signal bandwidth, and an azimuth resolution are related to the antenna aperture, while the radial velocity resolution is related to the radar coherent integration time.

The iterative search method can filter out all of the possible associated target measurements and combine them into one combination. Thus, all of the data are divided into several combinations. The method begins with any measurement from any sensor. Here, we use the i_{h}th HFSWR measurement as the beginning point to demonstrate the iterative search method. The main steps are as follows.

Step 1: In the HFSWR set, only one measurement $(z_{k,\,i_{\mathrm{h}}}^{\mathrm{h}})$ is defined. Furthermore, one empty set AIS set is defined.

Step 2: Record the number of elements in the AIS and HFSWR sets.

Step 3: Use every measurement in the HFSWR set, traverse all of the AIS measurements, find all of the AIS measurements that fall within the gating thresholds of Eq. (10), and then add them into the AIS set.

Step 4: Use every measurements in the AIS set, traverse all of the HFSWR measurements, find all of the HFSWR measurements that fall within the gating thresholds of Eq. (10), and then add them into HFSWR set.

Step 5: If the existing number of elements in the AIS and HFSWR sets are equal to the number of elements in Step 2, go to Step 6; otherwise, go to Step 2 and continue the iteration.

Step 6: The combination of the AIS and HFSWR sets represents the iterative search results.

After the iterative search, we can divide all of the measurements into different combinations. There are two types of combinations.

Type 1: The union of the AIS and HFSWR sets only contains the measurements of one sensor. This type is not considered in the cooperative target association.

Type 2: The union of the AIS and HFSWR sets contains the measurements from both sensors. These measurements can potentially originate from the cooperative vessels.

3.2 *JVC point association*

For each Type 2 combination, the JVC assignment algorithm is used to associate the HFSWR and AIS point targets. The JVC algorithm is usually used for global data association endeavors

(Malkoff, 1997; Sheng et al., 2010; Zhang et al., 2015). Here, we used the JVC algorithm to solve the point association problem.

The purpose of the JVC algorithm is to find the optimal association results in order to obtain the minimum sum of the assignment cost $c_{i_\mathrm{h}i_\mathrm{a}}$, which is defined as

$$J = \min \sum_{i_\mathrm{h}=0}^{i_\mathrm{h}=n_\mathrm{h}} \sum_{i_\mathrm{a}=0}^{i_\mathrm{a}=n_\mathrm{a}} d_{i_\mathrm{h}i_\mathrm{a}} c_{i_\mathrm{h}i_\mathrm{a}}, \tag{11}$$

subject to the following:

$$\sum_{i_\mathrm{h}=0}^{i_\mathrm{h}=n_\mathrm{h}} d_{i_\mathrm{h}i_\mathrm{a}} = 1 \quad \text{for } i_\mathrm{a} = 1,\ 2,\ \ldots,\ n_\mathrm{a}, \tag{12}$$

$$\sum_{i_\mathrm{a}=0}^{i_\mathrm{a}=n_\mathrm{a}} d_{i_\mathrm{h}i_\mathrm{a}} = 1 \quad \text{for } i_\mathrm{h} = 1,\ 2,\ \ldots,\ n_\mathrm{h}, \tag{13}$$

where $d_{i_\mathrm{h}i_\mathrm{a}} = \{0, 1\}$, is a binary function. A value of $d_{i_\mathrm{h}i_\mathrm{a}} = 1$ represents the association of the i_hth HFSWR point with the i_ath AIS point, whereas $d_{i_\mathrm{h}i_\mathrm{a}} = 0$ indicates that the two points are not associated. The assignment cost $c_{i_\mathrm{h}i_\mathrm{a}}$ is defined as follows:

$$c = \begin{bmatrix} c_{00} & c_{01} & c_{02} & \cdots & c_{0(n_a-1)} & c_{0n_a} \\ c_{10} & c_{11} & \cdots & \cdots & \cdots & c_{1n_a} \\ c_{20} & \vdots & & & \vdots & \vdots \\ \vdots & \vdots & & & \vdots & \vdots \\ c_{(n_h-1)0} & \vdots & & & \vdots & c_{(n_h-1)n_a} \\ c_{n_h0} & c_{n_h1} & \cdots & \cdots & c_{n_h(n_a-1)} & c_{n_hn_a} \end{bmatrix}. \tag{14}$$

Because of the existence of false alarms and non-cooperative targets, the HFSWR and AIS points are not always matched. Thus, a value of i_h=0 indicates that the corresponding AIS point has no associated HFSWR point, and a value of i_a=0 indicates that the corresponding HFSWR point has no associated AIS point.

In the point association process, the AIS points are treated as real targets, while the noise measurements of the HFSWR points are assumed to have a zero-mean Gaussian distribution. Here, the reciprocal of the HFSWR conditional probability is selected as the assignment cost. For i_h>0 and i_a>0, $c_{i_\mathrm{h}i_\mathrm{a}}$ is defined as follows:

$$c_{i_\mathrm{h}i_\mathrm{a}} = 1/P\left\{z^\mathrm{h}_{k,\,i_\mathrm{h}} / z^\mathrm{a}_{k,\,i_\mathrm{a}}\right\}. \tag{15}$$

The conditional probability for detection using HFSWR is defined as

$$P\left\{z^\mathrm{h}_{k,\,i_\mathrm{h}} / z^\mathrm{a}_{k,\,i_\mathrm{a}}\right\} = P\left[z^\mathrm{h}_{k,\,i_\mathrm{h}}(r) / z^\mathrm{a}_{k,\,i_\mathrm{a}}(r)\right] P\left[z^\mathrm{h}_{k,\,i_\mathrm{h}}(\theta) / z^\mathrm{a}_{k,\,i_\mathrm{a}}(\theta)\right] \times P\left[z^\mathrm{h}_{k,\,i_\mathrm{h}}(v) / z^\mathrm{a}_{k,\,i_\mathrm{a}}(v)\right], \tag{16}$$

where the probability of each vector is defined as follows:

$$P\left[z^\mathrm{h}_{k,\,i_\mathrm{h}}(r) / z^\mathrm{a}_{k,\,i_\mathrm{a}}(r)\right] = \int_{-\infty}^{z^\mathrm{h}_{k,\,i_\mathrm{h}}(r)} \frac{1}{\sqrt{2\pi}\sigma} \mathrm{e}^{-\frac{\left[t - z^\mathrm{a}_{k,\,i_\mathrm{a}}(r) - \Delta_k(r)\right]^2}{2\sigma^2}} \mathrm{d}t. \tag{17}$$

3.3 *Systematic bias derivation*

According to the results of association for the cooperative vessels at the time k, we can derive the HFSWR systematic bias at the time k. Because of the existence of systematic biases and measurement noise, the HFSWR measurements for the same target do not equal the AIS measurements. If the i_hth HFSWR measurement and the i_ath HFSWR measurement are associated with each other, we can derive

$$z^\mathrm{h}_{k,\,i_\mathrm{h}} - \Delta_k - w^\mathrm{h}_{k,\,i_\mathrm{h}} = z^\mathrm{a}_{k,\,i_\mathrm{a}}. \tag{18}$$

For n associated results at the time k,

$$\sum_{m=1}^{n} \left(z^\mathrm{h}_{k,\,i^m_\mathrm{h}} - \Delta_k - w^\mathrm{h}_{k,\,i^m_\mathrm{h}}\right) = \sum_{m=1}^{n} z^\mathrm{a}_{k,\,i^m_\mathrm{a}}, \tag{19}$$

where i^m_h represents the index of the HFSWR measurements for the mth association results. Furthermore, we can derive

$$\sum_{m=1}^{n} z^\mathrm{h}_{k,\,i^m_\mathrm{h}} - n \cdot \Delta_k - \sum_{m=1}^{n} w^\mathrm{h}_{k,\,i^m_\mathrm{h}} = \sum_{m=1}^{n} z^\mathrm{a}_{k,\,i^m_\mathrm{a}}. \tag{20}$$

If the number of cooperative associations is large, the measurement noise $\sum_{m=1}^{n} w^\mathrm{h}_{k,\,i^m_\mathrm{h}} \approx 0$. Therefore, we can estimate the HFSWR systematic bias by

$$\Delta_k = \frac{1}{n}\left(\sum_{m=1}^{n} z^\mathrm{h}_{k,i^m_\mathrm{h}} - \sum_{m=1}^{n} z^\mathrm{a}_{k,\,i^m_\mathrm{a}}\right), \tag{21}$$

and can be estimated as follows:

$$\sigma^2 = \frac{\sum_{m=1}^{n}\left(z^\mathrm{h}_{k,\,i^m_\mathrm{h}} - z^\mathrm{a}_{k,\,i^m_\mathrm{a}}\right)^2}{n-1}. \tag{22}$$

3.4 *Systematic bias estimation*

A systematic bias estimation algorithm is based on the association results for cooperative vessels. However, the HFSWR systematic biases are unknown during the point association process. Therefore, we must first suppose initial values for the HFSWR systematic biases and then use an iteration method to estimate the bias and covariance.

The values of the HFSWR systematic biases and covariance are initialized as follows: $\Delta^{(0)}_k(r) = 0$, $\Delta^{(0)}_k(\theta) = 0$, $\Delta^{(0)}_k(v) = 0$, $\sigma^{(0)}_k(r) = \frac{r_\mathrm{max}}{3}$, $\sigma^{(0)}_k(\theta) = \frac{\theta_\mathrm{max}}{3}$, $\sigma^{(0)}_k(v) = \frac{v_\mathrm{max}}{3}$, iteration time i=0, and ξ=[0.1 0.01 0.01].

Main iteration has three steps. Step 1: based on the supposed parameters $\Delta^{(i)}_k(r,\theta,v)$, $\sigma^{(i)}_k(r)$, $\sigma^{(i)}_k(\theta)$, and $\sigma^{(i)}_k(v)$, point measurements are associated using the JVC point association algorithm. Step 2: the systematic biases are derived as described in section 3.3 to obtain a temporary bias Δ^te_k and a temporary covariance σ^te_k. Step 3: if $\left|\Delta^{(i)}_k(r) - \Delta^\mathrm{te}_k(r)\right| \leqslant \xi(r)$, $\left|\Delta^{(i)}_k(\theta) - \Delta^\mathrm{te}_k(\theta)\right| > \xi(\theta)$, and $\left|\Delta^{(i)}_k(v) - \Delta^\mathrm{te}_k(v)\right| < \xi(v)$, go to Step 4. If $\left|\Delta^{(i)}_k(r) - \Delta^\mathrm{te}_k(r)\right| > \xi(r)$, the range bias is updated as follows:

$$\Delta^{(i+1)}_k(r) = \Delta^{(i)}_k(r) + (-1)^\delta \Delta^\mathrm{s}_k(r), \tag{23}$$

where $\Delta^\mathrm{s}_k(r) = \frac{1}{2}\left|\Delta^{(i)}_k(r) - \Delta^\mathrm{te}_k(r)\right|$, and δ is defined as follows:

$$\left.\begin{array}{ll}\delta=0 & \text{if} \quad \Delta_k^{(i)}(r) \geqslant \Delta_k^{\text{te}}(r) \\ \delta=1 & \text{if} \quad \Delta_k^{(i)}(r)<\Delta_k^{\text{te}}(r)\end{array}\right\}. \tag{24}$$

The range covariance is updated as

$$\sigma_k^{(i+1)}(r)=\frac{1}{3}\left(r_{\max}-\Delta_k^{(i+1)}(r)\right). \tag{25}$$

Similarly, the azimuth and radial velocity parameters are updated. Then, i=i+1. Go to Step 1. Step 4: $\Delta_k^{(i)}(r,\theta,v)$, $\sigma_k^{(i)}(r)$, $\sigma_k^{(i)}(\theta)$ and $\sigma_k^{(i)}(v)$ are the final estimated values.

4 Fusion JPDA-UKF vessel tracking algorithm

Following the estimation of the HFSWR biases, the dual-frequency biases can be corrected, after which the measurements at each frequency are mapped into the same level. Therefore, the dual-frequency measurements can all be used in the vessel tracking algorithm. The JPDA-UKF algorithm is effective for target tracking purposes. Here, we propose a fusion JPDA-UKF vessel tracking algorithm for the dual-frequency HFSWR data. In this algorithm, the dual-frequency measurements are employed as the point targets, and different frequencies are assigned with different weights. The measurements are fused in the measurement-to-track JPDA association process. The UKF is employed to estimate the states of the vessels. The fusion JPDA-UKF vessel tracking algorithm is introduced as follows.

(1) Track initiation: Two point estimates are used to initiate the tracks for both dual-frequency measurements.

(2) Position prediction: Based on the track, the vessel position at the next sample time is predicted using the dynamic model in Eq. (1), the measurement at the next sample time is predicted using Eq. (4), and the innovation vector of each track is updated.

(3) Data association: The measurement-to-track association is based on the JPDA framework. The association probabilities $\beta_{ij}^{f_1}$ and $\beta_{ij}^{f_2}$ are computed for each frequency following the literature (Maresca et al., 2014):

$$\beta_{ij}^{f_1} \equiv \left\{\begin{array}{ll}P\{\text{no measurement are origniated by } j\text{th vessel}\}, & i=0 \\ P\{i\text{th measurement are origniated by } j\text{th vessel}\}, & i\neq 0\end{array}\right., \tag{26}$$

$$\beta_{ij}^{f_2} \equiv \left\{\begin{array}{ll}P\{\text{no measurement are origniated by } j\text{th vessel}\}, & i=0 \\ P\{i\text{th measurement are origniated by } j\text{th vessel}\}, & i\neq 0\end{array}\right.. \tag{27}$$

where f_1 and f_2 represent the HFSWR working frequencies.

(4) Track update: for the Track j, the estimated state vector $\mathbf{X}_{k|k}^j$ at the Time k and the covariance $\boldsymbol{P}_{k|k}^j$ using feasible measurements at the Time k along Track j are updated as follows:

$$x_{k|k}^j = w_{f_1}\left[\beta_{0j}^{f_1}x_{k|k-1}^j+\sum_{i=1}^{m_j(k)}\beta_{ij}^{f_1}x_{k|k}^j(i)\right]+w_{f_2}\left[\beta_{0j}^{f_2}x_{k|k-1}^j+\sum_{i=1}^{m_j(k)}\beta_{ij}^{f_1}x_{k|k}^j(i)\right], \tag{28}$$

$$\begin{aligned}P_{k|k}^j = {} & w_{f_1}\left\{\beta_{0j}^{f_1}P_{k|k-1}^j+\sum_{i=1}^{m_j(k)}\beta_{ij}^{f_1}\left[P_{k|k}^j+\left(X_{k|k}^j(i)-X_{k|k}^j\right)\left(X_{k|k}^j(i)-X_{k|k}^j\right)^{\mathrm{T}}\right]\right\}+ \\ & w_{f_2}\left\{\beta_{0j}^{f_2}P_{k|k-1}^j+\sum_{i=1}^{m_j(k)}\beta_{ij}^{f_2}\left[P_{k|k}^j+\left(X_{k|k}^j(i)-X_{k|k}^j\right)\left(X_{k|k}^j(i)-X_{k|k}^j\right)^{\mathrm{T}}\right]\right\},\end{aligned} \tag{29}$$

where $\boldsymbol{X}_{k|k-1}^j$ is the state prediction with (k-1) measurements, $\boldsymbol{X}_{k|k}^j(i)$ is the UKF update using the ith validated measurement; and w_{f_1} and w_{f_2} are the weights of the dual-frequency measurements.

In this algorithm, we describe only the dual-frequency fusion process in the vessel tracking algorithm, while the other details of the JPDA and the UKF in the HFSWR tracking algorithm are referred to the work of Maresca et al. (2014).

5 Experimental results

In this section, real-life dual-frequency HFSWR and AIS vessel detection data are used to evaluate the performance of the proposed algorithm. The detection areas are located within the range of 37.0°–40.5°N and 118.5°–122°E. The experiment consists of two parts: the first is the test vessel tracking experiment, and the second is the multi-target vessel tracking experiment.

The HFSWR detection data of vessels are obtained from a coastal dual-frequency radar with working frequencies of 4.7 and 8.9 MHz. The radar point target sampling interval is 1 min. The HFSWR measurements are detected using the CFAR method through adaptive power regression thresholding (APRT) (Dzvonkovskaya and Rohling, 2007).

The AIS detection data are derived from AIS reports, which are acquired from the terrestrial AISs. For consistence with the radar data, we refreshed the AIS data with a sampling time of 1 min using the DR method.

5.1 *Single-target dual-frequency JPDA-UKF tracking experiment based on test vessels*

This section verifies the feasibility of the dual-frequency fusion JPDA-UKF tracking algorithm for the experimental vessel named *Yi Xing*. We use the route that the vessel sailed as our designed route, and we track it using the dual-frequency HFSWR. The shipping line of the experimental vessel is shown in Fig. 1, and the sailing time ranged from 06:01 to 18:30 on April 13th. The

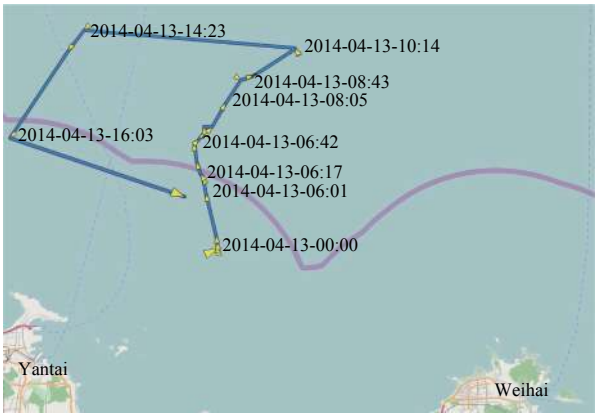

Fig. 1. Shipping line of the cooperative test ship.

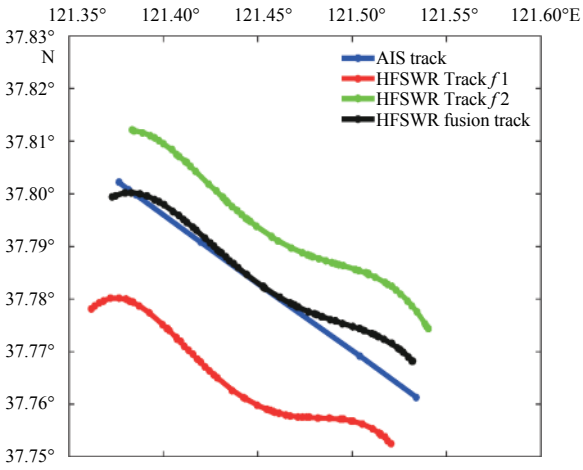

Fig. 2. Tracking results for the test vessel tracking different by using different frequencies.

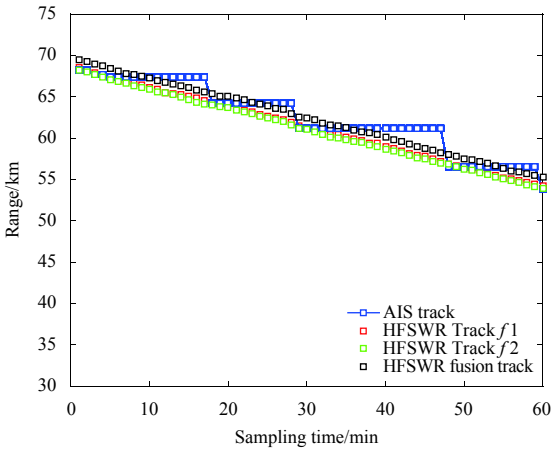

Fig. 3. Range results for tracking the test vessel at frequencies.

vessel target was tracked using the dual-frequency HFSWR over the course of an hour from 16:51:42 to 17:51:42.

The tracking results for the experimental vessel using different frequencies are shown in Fig. 2. Frequencies 1 and 2 and the fusion frequency can effectively track the test vessel, and the tracking results of the dual-frequency fusion detection agree more with the real AIS tracking data than the results obtained using single frequencies. The tracking results for the range, the azimuth and radial velocities using different frequencies are shown in Figs 3, 4 and 5, respectively. The mean tracking errors are shown in Table 1. The improvement in the azimuth error is the most obvious, while the improvements in the errors of the range and the radial velocity are relatively slight.

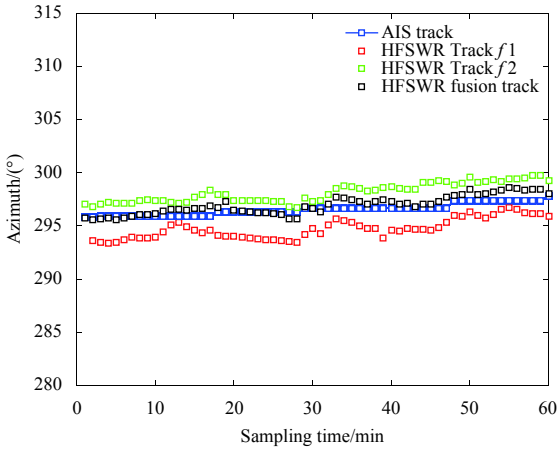

Fig. 4. Azimuth results for tracking the test vessel at different frequencies.

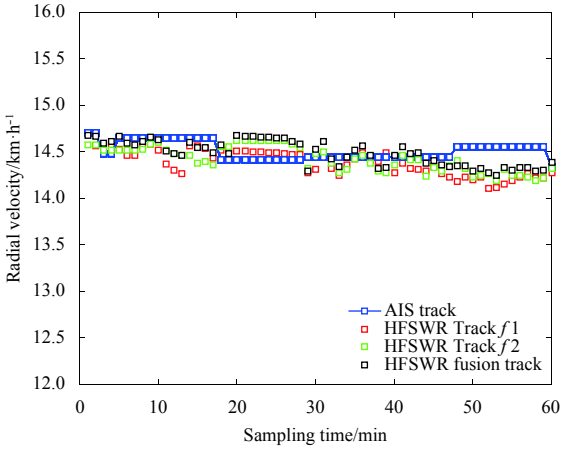

Fig. 5. Radial velocity results for tracking the test vessel at different frequencies.

5.2 *Multi-target dual-frequency JPDA -UKF tracking experiment*

In this section, multiple targets are tracked using the dual-frequency HFSWR. The detection areas are located within the range of 37.0°–40.5°N and 118.5°–122°E. The detection time ranged from 09:28:30 to 10:28:30 on September 6, 2013.

5.2.1 *Bias estimation*

The HFSWR systematic biases are estimated with the information of the cooperative vessels. We first associate the HFSWR measurements and the AIS measurements using the JVC point association algorithm. Then, we estimate the systematic biases using the systematic bias estimation algorithm.

The dual-frequency HFSWR system range, azimuth and radial velocity biases are highlighted in Fig. 6. From Fig. 6a, the value of the range bias is evidently small, and the range bias at Frequency 1 is higher than the range bias at Frequency 2. From Fig.

Table 1. Tracking performance of the test vessel

Evaluation metric	HFSWR *f*1	HFSWR *f*2	HFSWR fusion
Mean range error/km	0.46	0.42	0.36
Mean azimuth error/(°)	3.21	1.56	1.23
Mean radial velocity error/km·h^{-1}	0.56	0.39	0.40

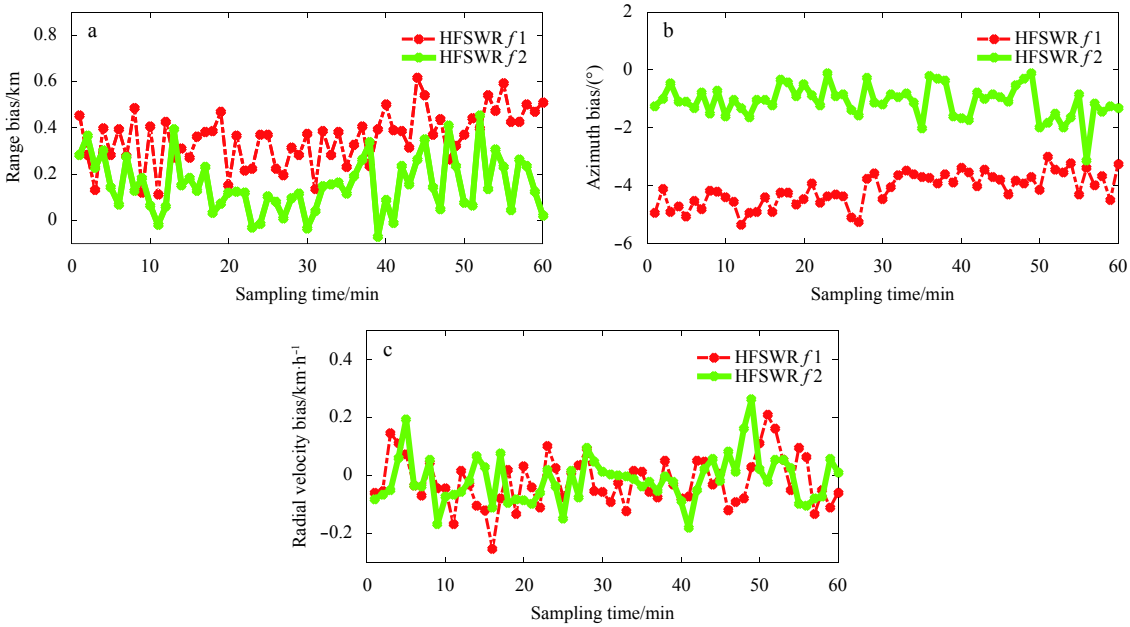

Fig. 6. Range, azimuth, and radial velocity bias estimations for the HFSWR measurements.

6b, we can observe that the azimuth bias at Frequency 1 is approximately –5° and that the azimuth bias at Frequency 2 is approximately –2°. From Fig. 6c, the radial velocity bias is also clearly small.

5.2.2 *Bias correction analyses for the tracking of cooperative vessels*

To analyze the HFSWR systematic bias correction results, the cooperative vessel is tracked to verify the correction results of the HFSWR point targets. AIS tracking results for the cooperative vessel are extracted from the AIS measurements. The corresponding HFSWR radar points are selected using the gating thresholds and the nearest neighbor method.

A comparison between the range values of the AIS tracking points and the corresponding HFSWR points is shown in Fig. 7. The blue circles represent the AIS tracking point targets, and the red circles represent the point targets at the HFSWR Frequency 1, while the red squares represent the corrected point targets at the HFSWR Frequency 1. The green points represent the point targets at the HFSWR Frequency 2. Missing HFSWR points may have been missed during the radar detection process. In Fig. 7, the corrected HFSWR points are closer to the AIS data.

A comparison between the azimuth values of the AIS tracking points and the corresponding HFSWR points is shown in Fig. 8.

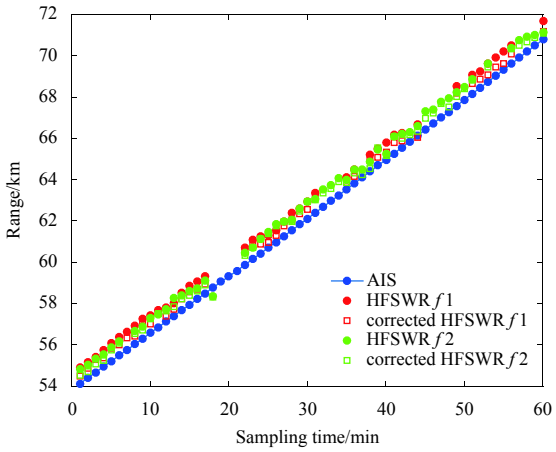

Fig. 7. Comparison of the range within the cooperative vessel measurements.

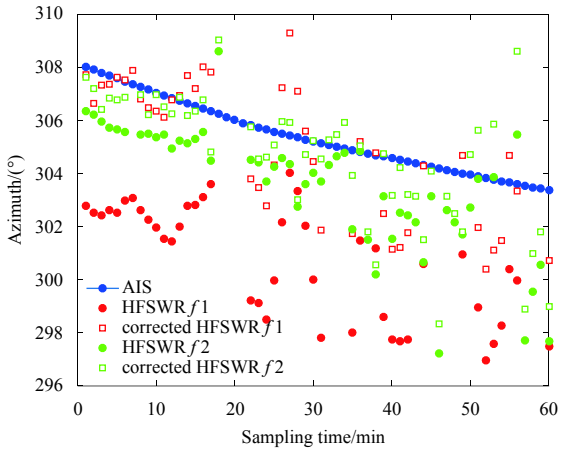

Fig. 8. Comparison of the azimuth within the cooperative vessel measurements.

From Fig. 8, the azimuth values of the HFSWR points have high biases compared with those of the AIS points. The corrected dual-frequency HFSWR points are closer to each other and to the AIS points. The corrected results are more useful for the fusion of the dual-frequency HFSWR points. Figure 9 compares the radial velocities of the AIS tracking points with the corresponding HFSWR points. The corrected velocity results indicate that the radial velocity cannot improve the accuracy naturally.

5.2.3 *JPDA-UKF tracking*

To verify the effects of the JPDA-UKF tracking algorithm, ten cooperative vessels are tracked in this section. Figure 10 shows the results of AIS tracking of the ten vessels examined in the experiment. The vessels are tracked using HFSWR Frequencies 1 and 2 in addition to HFSWR dual-frequency fusion data. Tracking using the HFSWR fusion method is conducted based on the systematically bias-corrected HFSWR data.

The mean range, azimuth and radial velocity errors are used to evaluate the performances of the tracking algorithms, which are defined as follows:

$$\bar{\varepsilon} = \frac{1}{N_{\rm tr} \cdot t_{\rm tr}} \sum_{j=1}^{N_{\rm tr}} \left\{ \sum_{k=1}^{t_{\rm tr}} \left[z_k^{\rm h}(j) - z_k^{\rm a}(j) \right] \right\}, \tag{30}$$

where $z_k^{\rm h}(j)$ is the measurement value of Track j, which is transformed from the position at the time k; $z_k^{\rm a}(j)$ is the AIS point value of Track j, $N_{\rm tr}$ is the number of the true track, where only unmissed tracks are considered as true tracks; and $t_{\rm tr}$ is the tracking time.

The tracking performances of the ten vessels are highlighted in Table 2. The fusion JPDA-UKF vessel tracking algorithm can provide lower mean errors and higher tracking capabilities than tracking using a single frequency. All of the 10 tracks are tracked using the dual-frequency algorithm, while Tracks 2 and 3 are lost during the tracking processes using Frequencies 1 and 2, respectively.

Tracks 1 and Track 2 are selected to demonstrate the tracking details. Among these tracks, Track 1 is a vessel sailing away from the station, while Track 2 is a vessel sailing toward the radar station. The vessel tracking results using the HFSWR Frequencies 1 and 2 and HFSWR dual-frequency fusion data are shown in Figs 11, 12 and 13 for the range, the azimuth, and the radial velocity, respectively. The corresponding AIS tracks are also labeled in the figures to verify the tracking effects.

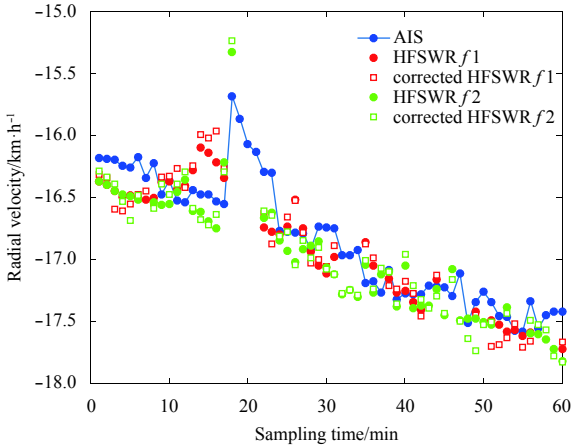

Fig. 9. Comparison of the radial velocity within the cooperative vessel measurements.

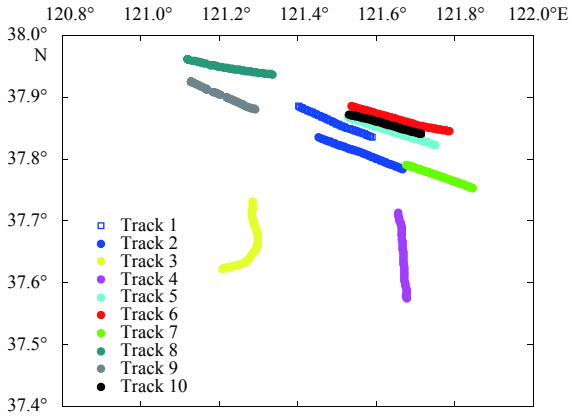

Fig. 10. AIS tracking results for the ten vessels.

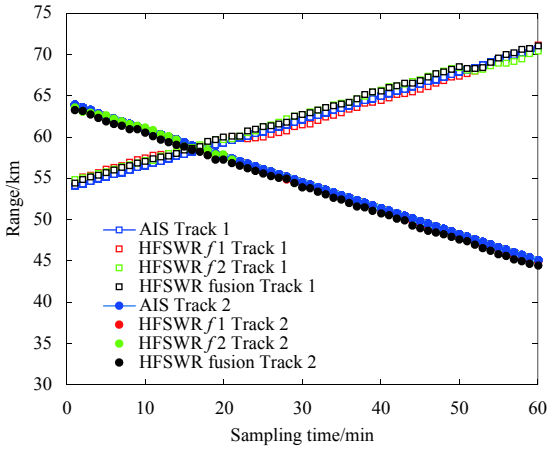

Fig. 11. Range results during vessel tracking at different frequencies.

During the initial stages in Figs 11–13, the tracking results at Frequency 2 are closer to the AIS tracking data. However, Track 2 is missed using Frequency 2 when the sampling time is 20 min. The tracking process using the HFSWR fusion method can provide higher tracking accuracies than the tracking processes with single frequency. The errors in the range and radial velocity for the three tracking methods are all small, while the error in the azimuth is relatively large.

Table 2. Tracking performances for the ten vessels

Evaluation matric	HFSWR *f*1	HFSWR *f*2	HFSWR fusion
Mean range error/km	0.54	0.65	0.49
Mean azimuth error/(°)	3.49	1.98	1.86
Mean radial velocity error/km·h^{-1}	0.43	0.39	0.26
Number of tracking targets lost	2	3	0

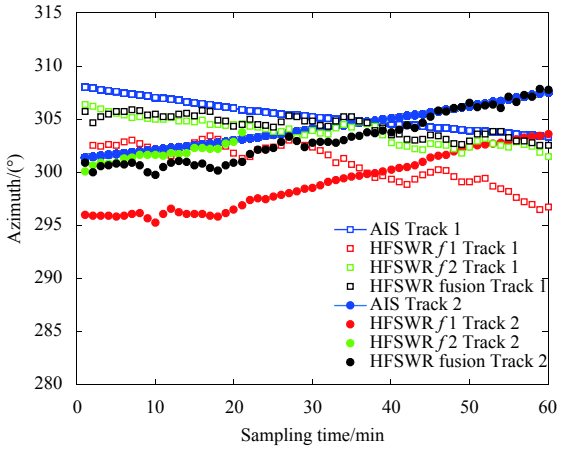

Fig. 12. Azimuth results during vessel tracking at different frequencies.

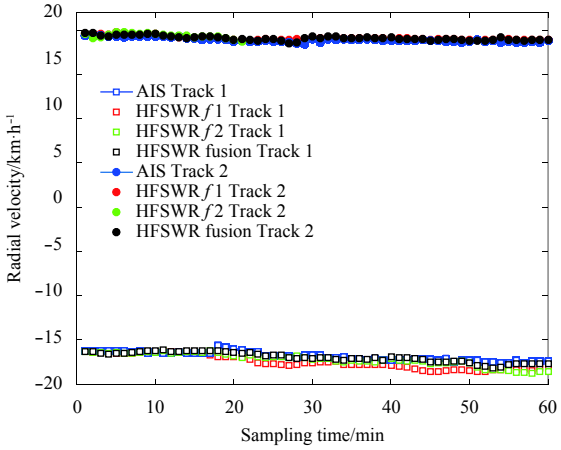

Fig. 13. Radial velocity results during vessel tracking at different frequencies.

6 Conclusions

Tracking a marine vessel with the dual-frequency HFSWR data can improve the tracking capability and accuracy. Since the HFSWR systematic biases are different for different frequencies, the dual-frequency tracking processes are traditionally conducted through the implementation of tracking association and tracking fusion. In this paper, we propose a new vessel fusion tracking procedure with dual-frequency HFSWR incorporating an AIS calibration technology. The measurements of the cooperative vessel are used to evaluate the HFSWR systematic biases. After the biases are corrected, a dual-frequency fusion JPDA-UKF algorithm is applied to track the vessel. The experimental results of real-life detection data show that the proposed method cannot only track the vessels in real time but also improve the tracking accuracy compared with the tracking processes involving single-frequency data. However, with an increase in the number of tracking targets, the tracking time will grow immensely, primarily because the JPDA algorithm is time consuming. When the number of tracking targets is increased, this method is unable to track all of the targets in 1 min with the computer used in this study (Intel i3-3220CPU, 16G RAM). Future research will concentrate on improving the efficiency of the tracking algorithm and reducing the tracking time.

References

Bar-Shalom Y, Li Xiaorong. 1995. Multitarget-Multisensor Tracking: Principles and Techniques. Storrs, CT: YBS Publishing

Braca P, Grasso R, Vespe M, et al. 2012. Application of the JPDA-UKF to HFSW radars for maritime situational awareness. In: Proceedings of 15th International Conference on Information Fusion (FUSION). Singapore: IEEE, 2585–2592

Braca P, Maresca S, Grasso R, et al. 2015. Maritime surveillance with multiple over-the-horizon HFSW radars: an overview of recent experimentation. IEEE Aerospace and Electronic Systems Magazine, 30(12): 4–18

Bruno L, Braca P, Horstmann J, et al. 2013. Experimental evaluation of the range-doppler coupling on HF surface wave radars. IEEE Geoscience and Remote Sensing Letters, 10(4): 850–854

Chaturvedi S K, Yang C, Ouchi K, et al. 2012. Ship recognition by integration of SAR and AIS. Journal of Navigation, 65(02): 323–337

Dzvonkovskaya A, Gurgel K W, Rohling H, et al. 2008. Low power high frequency surface wave radar application for ship detection and tracking. In: Proceedings of 2008 International Conference on Radar. Adelaide, SA: IEEE, 627–632

Dzvonkovskaya A L, Rohling H. 2007. Ship detection with adaptive power regression thresholding for HF radar. Radar Science and Technology, 5(2): 81–85

Dzvonkovskaya A L, Rohling H. 2010. HF radar performance analysis based on AIS ship information. In: Proceedings of 2010 IEEE Radar Conference. Washington, DC: IEEE, 1239–1244

Grosdidier S, Baussard A, Khenchaf A. 2010. HFSW radar model: simulation and measurement. IEEE Transactions on Geoscience and Remote Sensing, 48(9): 3539–3549

Gurgel K W, Schlick T, Horstmann J, et al. 2010. Evaluation of an HF-radar ship detection and tracking algorithm by comparison to AIS and SAR data. In: Proceedings of 2010 International Waterside Security Conference (WSS). Carrara: IEEE, 1–6

Habtemariam B, Tharmarasa R, McDonald M, et al. 2015. Measurement level AIS/radar fusion. Signal Processing, 106: 348–357

Ince A N, Topuz E, Panayirci E, et al. 1998. Principles of Integrated Maritime Surveillance Systems. New York: Springer

Ji Yonggang, Zhang Jie, Meng Junmin, et al. 2014a. Point association analysis of vessel target detection with SAR, HFSWR and AIS. Acta Oceanologica Sinica, 33(9): 73–81

Ji Yonggang, Zhang Jie, Wang Yiming, et al. 2014b. Ship detection point association and fusion with dual-frequency HF surface wave radar. Systems Engineering and Electronics (in Chinese), 36(2): 266–271

Ji Yonggang, Zhang Jie, Wang Yiming, et al. 2016. Vessel target detection based on fusion range-Doppler image for dual-frequency high-frequency surface wave radar. IET Radar, Sonar & Navigation, 10(2): 333–340

Malkoff D B. 1997. Evaluation of the Jonker-Volgenant-Castanon (JVC) assignment algorithm for track association. In: Proceedings Volume 3068, Signal Processing, Sensor Fusion, and Target Recognition VI. Orlando, FL, United States: SPIE, 228–239

Maresca S, Braca P, Horstmann J, et al. 2014. Maritime surveillance using multiple high-frequency surface-wave radars. IEEE Transactions on Geoscience and Remote Sensing, 52(8): 5056–5071

Ponsford T, Wang Jian. 2010. A review of high frequency surface wave radar for detection and tracking of ships. Turkish Journal of Electrical Engineering & Computer Sciences, 18(3): 409–428

Sheng Weidong, Lin Liangkui, An Wei, et al. 2010. A passive multisensor multitarget track association algorithm based on global optimization. Journal of Electronics & Information Technology (in Chinese), 32(7): 1621–1625

Vivone G, Braca P, Horstmann J. 2015. Knowledge-based multitarget ship tracking for HF surface wave radar systems. IEEE Transactions on Geoscience and Remote Sensing, 53(7): 3931–3949

Xiao F, Ligteringen H, Van Gulijk C, et al. 2015. Comparison study on AIS data of ship traffic behavior. Ocean Engineering, 95(0): 84–93

Xiong Kai, Zhang Hongyue, Chan C W. 2006. Performance evaluation

of UKF-based nonlinear filtering. Automatica, 42(2): 261–270

Zhang Hui, Liu Yongxin, Zhang Jie, et al. 2015. Target point tracks optimal association algorithm with surface wave radar and automatic identification system. Journal of Electronics & Information Technology (in Chinese), 37(3): 619–624

Zhou Yifeng, Leung H, Blanchette M. 1999. Sensor alignment with earth-centered earth-fixed (ECEF) coordinate system. IEEE Transactions on Aerospace and Electronic Systems, 35(2): 410–418

Zhou Yifeng, Leung H, Yip P C. 1997. An exact maximum likelihood registration algorithm for data fusion. IEEE Transactions on Signal Processing, 45(6): 1560–1573